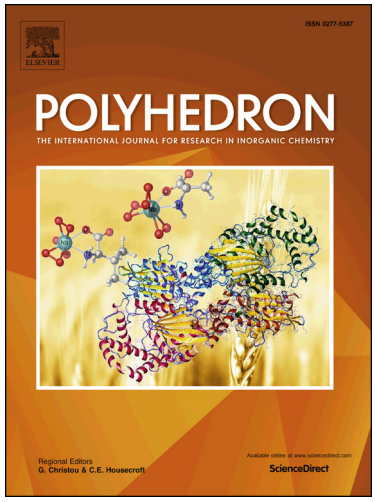

Synthesis, photoluminescence properties of novel cationic Ir(III) complexes with phenanthroimidazole derivative as the ancillary ligand

Fuzhi Yang, Tianzhi Yu, Yuling Zhao, Hui Zhang, Yuying Niu

PII: S0277-5387(17)30591-0
DOI: https://doi.org/10.1016/j.poly.2017.09.014
Reference: POLY 12824

To appear in: *Polyhedron*

Received Date: 20 July 2017
Accepted Date: 13 September 2017

Please cite this article as: F. Yang, T. Yu, Y. Zhao, H. Zhang, Y. Niu, Synthesis, photoluminescence properties of novel cationic Ir(III) complexes with phenanthroimidazole derivative as the ancillary ligand, *Polyhedron* (2017), doi: https://doi.org/10.1016/j.poly.2017.09.014

Synthesis, photoluminescence properties of novel cationic Ir(III) complexes with phenanthroimidazole derivative as the ancillary ligand

Fuzhi Yang[1], Tianzhi Yu[1,*], Yuling Zhao[2], Hui Zhang[1], Yuying Niu[1]

[1]Key Laboratory of Opto-Electronic Technology and Intelligent Control (Ministry of Education), Lanzhou Jiaotong University, Lanzhou 730070, China

[2]School of Chemical and Biological Engineering, Lanzhou Jiaotong University, Lanzhou 730070, China

Abstract: Two novel cationic Ir(III) complexes, **[(nbt)$_2$Ir(L)](PF$_6$)** and **[(CF$_3$-bt)$_2$Ir(L)](PF$_6$)**, where **nbt** = 2-(1-naphthyl)benzothiazole; **CF$_3$-bt** = 2-phenyl-6-(trifluoromethyl)-benzothiazole and **L** = 1-(4-(*tert*-butyl)phenyl)-2-(5-(9-(*p*-tolyl)-9*H*-carbazol-3-yl)pyridin-2-yl)-1*H*-phenanthro [9,10-*d*]imidazole, were successfully synthesized and characterized. The structures of **L** and **[(nbt)$_2$Ir(L)](PF$_6$)** were confirmed by single crystal X-ray diffraction. Their photophysical, electrochemical properties and thermal stabilities were investigated systematically. The results showed that the Ir(III) complexes had higher thermal stabilities, and exhibited strong red emission and orange emission, respectively.

Keywords: Cationic Ir(III) complex; Phenanthroimidazole derivative; Crystal structure; Photoluminescence

[*]Corresponding Author. Tel. +86-931-4956935; Fax: +86-931-4938756; e-mail: yutzh@mail.lzjtu.cn (T.Z. Yu)

1. Introduction

In the last decades, the neutral Ir(III) complexes have been widely used as phosphorescent emitters in organic light-emitting diodes (OLEDs) due to their high phosphorescent efficiencies and tunable emission color [1-9]. However, the OLEDs based on Ir(III) complexes are highly sensitive to the doping concentration and devices suffer from reduced emission efficiency while increasing the concentration of phosphorescent emitters, thus Ir(III) complexes as electroluminescent (EL) materials are always doped in the host materials at appropriate concentration to fabricate OLEDs. In addition, the use of neutral Ir(III) complexes in OLEDs requires a complicated multilayered structure for charge injection, transport, and light emission [10-12].

Recently, the use of cationic iridium(III) complexes has attracted tremendous attentions due to their ability to be used in bio-imaging [13], light-emitting electrochemical cells (LECs) [14-16] as well as OLEDs [17-20]. Compared to the iridium(III) complexes, the cationic iridium complexes have many advantages such as easy preparation, facile tuning of the emission and the energy levels via the ancillary ligands, and good solubility in polar solvents. Moreover, the presence of mobile counter ions in the cationic Ir(III) complexes can form accumulation of negative charge near one electrode under applied voltage, which causes high electric fields at the electrodes, thus minimizing carrier injection barrier for electron and hole and enhancing electronic charge injection ultimately allowing for the use of a single-layer architecture operating at low voltages [21,22]. However, the large size of the cations renders the complexes to be essentially stationary in the device, meaning that upon initial application of a bias, the cation density at the cathode is initially much lower than the anion concentration at the anode, leading to an imbalance of charge injection into the device. By

doping in small amounts of alkali metal cation hexafluorophosphate salts (e.g., $LiPF_6$), it could lead to more balanced charge injection that ultimately improved not just response times, but also luminance values and EQEs [23]. In the current research state of cationic Ir(III) complexes, the OLEDs based on the cationic Ir(III) complexes have current efficiencies in the 12-31 cd/A range, much inferior to the neutral Ir(III) complexes based OLEDs [17,24-28]. For example, the Cao group reported highly efficient polymer light-emitting diodes based on yellow-green light-emitting cationic Ir(III) complexes with 1,10-phenanthroline derivatives containing oxadiazole-triphenylamine, oxadiazole or triphenylamine unit as neutral auxiliary ligands, in which the devices fabricated from the cationic Ir(III) complex containing bipolar unit of oxadiazole-triphenylamine exhibited higher EL performance with the maximum luminance efficiency of 30.6 cd/A and the maximum external quantum efficiency of 1.02% due to its balance of hole and electron fluxes [17]. Wong et al. [24] reported OLEDs based on sublimable cationic iridium complexes with rigid pyridinylfluorene derivatives as dopants, the devices exhibited yellow light emission with a maximum luminance efficiency of 20 cd/A and a quantum efficiency of 7%.

Benzimidazole derivatives have good luminescent and electron-transporting properties, and strong coordination ability to transition metal ions. In especial, 2-(2'-pyridyl)benzimidazole and its derivatives have aroused considerable interest due to their structural similarity to the widely studied 2,2'-bipyridine, 1,10-phenanthroline, 2,2'-biimidazole, etc., in containing the –N=C–C=N– group. Thus they have been often used as the powerful bidentate chelating agents to form stable luminescent complexes with various transition metal ions [29-31]. In previous studies we have reported the synthesis, crystal structures and luminescent properties of Cu(I) and Ln(III) complexes

with 1-substituted pyridyl benzimidazole ligands containing carbazole or oxadiazole unit [32-34]. As part of our continuous research interests in the metal complexes based on the functionalized benzimidazole ligands, in this paper a phenanthroimidazole derivative was synthesized as the neutral auxiliary ligand to prepare two new cationic Ir(III) complexes. The photophysical, electrochemical properties and thermal stabilities of the cationic Ir(III) complexes were reported.

The synthetic routes of the neutral auxiliary ligand **L** and the cationic Ir(III) complexes were shown in Scheme 1.

2. Experimental

2.1 Materials and methods

Carbazole and *p*-Iodotoluene were purchased from Shanghai Zhongqin Chemical Reagent Co. Ltd (China). 5-Bromopicolinaldehyde, phenanthrene-9,10-dione, 4-(tert-butyl)aniline, tetrabutyl ammonium bromide (TBAB), bis(pinacolato)diboron, tetrakis(triphenylphosphine)palladium ($Pd(PPh_3)_4$) and [1,1'-bis(diphenylphosphino)ferrocene]dichloropalladium(II) ($PdCl_2(dppf)$) were obtained from Energy Chemical (China). *N*-bromobutanimide (NBS), piperidine and 1,10-phenanthroline were bought from Tianjing Chemical Reagent Co. Ltd (China). All the other chemicals were analytical grade reagent. All of the organic solvents used in this study were dried over appropriate drying agents and freshly distilled prior in the related reaction.

^{1}H NMR spectra were recorded on Varian Mercury Plus 400 MHz and Agilent Technologies DDZ 600 MHz. Mass spectra were recorded using a Thermo Scientific Orbitrap Elite mass spectrometer. Thermogravimetric analysis (TGA) was performed on a PerkinElmer Pyris system.

UV-vis absorption and photoluminescent spectra were recorded on a Shimadzu UV-2550 spectrometer and on a Perkin-Elmer LS-55 spectrometer, respectively. Cyclic voltammetry (CHI Instruments 760 B) was performed with a 0.10 mol/L solution of tetrabutylammonium hexafluorophosphate (Bu_4NPF_6) in dichloromethane, with the analyte present in a concentration of 10^{-3} mol/L and employing a scan rate of 50 mV/s at room temperature. A glassy carbon electrode was used as the working electrode, while a Pt wire and an Ag/Ag^+ electrode were used as the counter electrode and reference electrode, respectively.

The cyclometalated Ir(III) μ-chlorobridged dimer of **$(nbt)_2Ir(\mu\text{-}Cl)_2Ir(nbt)_2$** was prepared as previously described [35]. The cyclometalated Ir(III) μ-chlorobridged dimer of **$(CF_3\text{-}bt)_2Ir(\mu\text{-}Cl)_2Ir(CF_3\text{-}bt)_2$** was synthesized according to the procedure described in the literature [36].

2.2 Synthesis and characterization of the ancillary ligand (L) and the cationic Ir(III) complexes

9-(*p*-Tolyl)-9*H*-carbazole: Carbazole (5.0 g, 29.90 mmol), 4-iodotoluene (7.82 g, 35.89 mmol) and potassium hydroxide (2.52 g, 44.91 mmol) were dissolved in *p*-xylene (100 mL), stirring for 1 h under the protection of nitrogen. Then 1,10-phenanthroline (0.27 g, 1.50 mmol) and CuI (0.285 g, 1.495 mmol) were added, after reacting 30 minutes, slowly heated to reflux for 48 h. The reaction mixture was cooled to room temperature and filtrated. The extracted solution was extracted with dichloromethane (3× 100 mL). The combined organic layer was dried by anhydrous $MgSO_4$ and concentrated under reduced pressure. The residue was purified by column chromatography on silica gel using petroleum ether as eluent to give the white product (9-*p*-tolyl-9*H*-carbazole) (6.93 g, 90%).

^{1}HNMR (400 MHz, $CDCl_3$, δ, ppm): 8.14 (d, *J* = 8.2 Hz, 2H, Ar-H), 7.43 (d, *J* = 8.0 Hz, 2H, Ar-H), 7.39 (d, *J* = 7.8 Hz, 4H, Ar-H), 7.27 (t, *J* = 7.8 Hz, 4H, Ar-H), 2.48 (s, 3H, -CH_3).

3-Bromo-9-(*p*-tolyl)-9*H*-carbazole: 3.00 g (11.66 mmol) of 9-*p*-tolyl-9*H*-carbazole was dissolved in absolute dichloromethane (20 mL). Under the ice bath, 2.08 g (11.69 mmol) of NBS dissolved in 40 mL of absolute dichloromethane was dropwise added in the reaction mixture, then the reaction mixture was stirred for overnight at room temperature. After the reaction was finished, the mixture was poured into 100 mL of water and extracted with dichloromethane (3× 100 mL), and then the combined organic layer was dried by anhydrous $MgSO_4$ and concentrated under reduced pressure. The residue was purified by column chromatography on silica gel using dichloromethane/petroleum ether (1:80, v/v) as eluent to obtain oyster white powder (3.72 g, 94.9%). m.p.: 136-138 ^oC. ^{1}H NMR (400 MHz, $CDCl_3$, δ, ppm): 8.24 (s, 1H, Ar-H), 8.08 (d, *J* = 8.0 Hz, 1H, Ar-H), 7.48-7.34 (m, 6H, Ar-H), 7.30-7.22 (m, 3H, Ar-H), 2.49 (s, 3H, -CH_3).

3-(4,4,5,5-tetramethyl-1,3,2-dioxaborolan-2-yl)-9-(*p*-tolyl)-9*H*-carbazole (I): 3-Bromo-9-(*p*-tolyl)-9*H*-carbazole (1.90 g, 5.65 mmol), bis(pinacolato)diboron (2.30 g, 9.06 mmol), $PdCl_2$(dppf) (0.20 g, 0.27 mmol) and potassium acetate (1.78 g, 18.14 mmol) were mixed in 60 mL of 1,4-dioxane solution. The mixture was stirred vigorously for 48 h under nitrogen atmosphere at 85 ^oC. After cooling, the reaction mixture was poured into cold water (300 mL), and extracted with dichloromethane (100 mL × 3). The combined organic phase was dried over anhydrous Na_2SO_4. After filtering, the filtrate was evaporated to dryness under reduced pressure. The crude was purified by chromatography on silica gel using petroleum ether/dichloromethane (3:1, v/v) as the eluent to give yellow powder (1.09 g, 50.3 %). ^{1}H NMR (400 MHz, $CDCl_3$, δ, ppm): 8.64 (s, 1H,

Ar-H), 8.17 (d, *J* = 8 Hz, 1H, Ar-H), 7.85 (d, *J* = 9.6 Hz, 1H, Ar-H), 7.43-7.24 (m, 8H, Ar-H), 2.48 (s, 3H, Ar-CH_3), 1.40 (s, 12H, -CH_3).

5-(9-(*p*-tolyl)-9*H*-carbazol-3-yl)picolinaldehyde (II): The compound **I** (1.00 g, 2.61 mmol), 5-bromopicolinaldehyde (0.53 g, 2.85 mmol), $Pd(pph_3)_4$ (0.15 g, 0.13 mmol), Na_2CO_3 (0.83 g, 7.83 mmol), TBAB (0.04 g, 0.124 mmol) and distilled water (4 mL) were mixed in 60 mL of toluene, and the mixture was stirred vigorously at 110 ^oC for 24 h. After cooling, a small quantity of water was added, and the mixture was extracted with dichloromethane (50 mL × 3). The organic phase was dried over anhydrous Na_2SO_4. After filtering, the filtrate was evaporated to dryness under reduced pressure. The crude was purified by chromatography on silica gel using dichloromethane/ethyl acetate (10:1, v/v) as the eluent to give pale yellow powder (0.76 g, 80.38 %). ^1H NMR (400 MHz, $CDCl_3$, δ, ppm): 10.15 (s, 1H, -CHO), 9.14 (s, 1H, Ar-H), 8.43 (s, 1H, Ar-H), 8.19 (dd, *J* = 7.2 Hz, J = 8.8 Hz, 2H, Ar-H), 8.06 (d, *J* = 8.0 Hz, 1H, Ar-H), 7.68 (d, *J* = 8.0 Hz, 1H, Ar-H), 7.50-7.40 (m, 7H, Ar-H), 7.34 (t, *J* = 6.8 Hz, 1H, Ar-H), 2.51 (s, 3H, Ar-CH_3).

1-(4-(*tert*-butyl)phenyl)-2-(5-(9-(*p*-tolyl)-9*H*-carbazol-3-yl)pyridin-2-yl)-1*H*-phenanthro[9, 10-*d*]imidazole (L): The compound **II** (1.21 g, 3.34 mmol), 9,10-phenanthrenequinone (0.70 g, 3.36 mmol), 4-(tert-butyl)aniline (0.8 mL, 5.02 mmol) and ammonium acetate (3.15 g, 40.87 mmol) were mixed in 120 mL of acetic acid and stirred vigorously for 12 h at 120 ℃. After cooling, the reaction mixture was poured into cold water (200 mL), and extracted with dichloromethane (150 mL × 3). The combined organic phase was dried over anhydrous Na_2SO_4. After filtering, the filtrate was evaporated to dryness under reduced pressure. The crude was purified by chromatography on silica gel using petroleum ether/ethyl acetate (2:1, v/v) as the eluent to obtain white solid product

(1.23 g, 54 %). m.p.: 259-262 ^{o}C. ^{1}H NMR (400 MHz, $CDCl_3$, δ, ppm): 8.95 (d, *J* = 8.0 Hz, 1H, Ar-H), 8.80 (s, 1H, Ar-H), 8.76 (d, *J* = 8.4 Hz, 1H, Ar-H), 8.70 (d, *J* = 8.0 Hz, 1H, Ar-H), 8.33 (s, 1H, Ar-H), 8.17 (d, *J* = 7.6 Hz, 1H, Ar-H), 8.06 (d, *J* = 8.4 Hz, 1H, Ar-H), 7.99 (d, *J* = 8.0 Hz, 1H, Ar-H), 7.75 (t, *J* = 7.6 Hz, 1H), 7.69-7.59 (m, 4H, Ar-H), 7.53-7.49 (m, 3H, Ar-H), 7.45-7.38 (m, 8H, Ar-H), 7.32-7.24 (m, 3H, Ar-H), 7.19 (d, *J* = 8.0 Hz, 1H, Ar-H), 2.49 (s, 3H, Ar-CH_3), 1.46 (s, 9H, -CH_3). ^{13}C NMR (100 MHz, $CDCl_3$, δ, ppm): 152.54, 149.38, 147.64, 147.47, 141.56, 140.98, 137.67, 137.51, 136.77, 136.43, 134.69, 134.25, 130.55, 129.56, 129.11, 128.89, 128.45, 128.39, 127.35, 127.21, 126.89, 126.46, 126.35, 126.23, 125.62, 125.02, 124.31, 124.00, 123.26, 123.08, 122.90, 121.29, 120.37, 120.13, 118.78, 110.41, 110.01, 34.97, 31.42, 21.25. HR EI-MS: Calcd. for $C_{49}H_{38}N_4$, 682.31; Found: 683.32 $[M+1]^+$.

$[(nbt)_2Ir(L)](PF_6)$: The chloro-bridged dimer complex **$(nbt)_2Ir(\mu\text{-}Cl)_2Ir(nbt)_2$** (0.30 g, 0.20 mmol) and **L** (0.27 g, 0.40 mmol) were refluxed in 60 mL of dichloromethane/methanol (1:1, v/v) under nitrogen atmosphere at 75 ℃ for 4 h with keeping in dark place. After cooling, an excess of KPF_6 (0.07 g, 0.38 mmol) was added and the mixture was stirred for 2 h at room temperature. After completion of the reaction, the solids in the solution were removed by filtration. The residue was purified through chromatography on silica gel using ethyl acetate/petroleum ether (3: 1, v/v) as the eluent to obtain the target product as a yellow solid (0.25 g, 40.48%). ^{1}H NMR (600 MHz, $CDCl_3$, δ, ppm): 8.92 (d, *J* = 8.8 Hz, 1H, Ar-H), 8.60 (d, *J* = 8.4 Hz, 1H, Ar-H), 8.48 (s, 1H, Ar-H), 8.32 (d, *J* = 8.4 Hz, 1H, Ar-H), 8.27 (d, *J* = 8.8 Hz, 1H, Ar-H), 8.18 (d, *J* = 8.6 Hz, 1H, Ar-H), 8.07 (d, *J* = 8.4 Hz, 1H, Ar-H), 7.93-7.89 (m, 3H, Ar-H), 7.85-7.82 (m, 3H, Ar-H), 7.75 (t, *J* = 7.2 Hz, 2H, Ar-H), 7.68 (s, 1H, Ar-H), 7.64 (d, *J* = 8.4 Hz, 1H, Ar-H), 7.60-7.55 (m, 2H, Ar-H), 7.52 (t, *J* = 7.2 Hz, 1H,

Ar-H), 7.47 (t, *J* = 7.8 Hz, 1H, Ar-H), 7.43-7.35 (m, 9H, Ar-H), 7.33 (d, *J* = 7.8 Hz, 1H, Ar-H), 7.31-7.27 (m, 4H, Ar-H), 7.25-7.20 (m, 3H, Ar-H), 7.15 (d, *J* = 8.8 Hz, 1H, Ar-H), 6.92 (t, *J* = 7.8 Hz, 1H, Ar-H), 6.83 (dd, *J* = 7.8, 8.4 Hz, 2H, Ar-H), 6.69 (d, *J* = 8.4 Hz, 1H, Ar-H), 6.47 (d, *J* = 8.4 Hz, 1H, Ar-H), 6.17 (t, *J* = 7.8 Hz, 1H, Ar-H), 6.08 (d, *J* = 8.4 Hz, 1H, Ar-H), 2.47 (s, 3H, Ar-CH_3), 1.52 (s, 9H, -CH_3). ^{13}C NMR (150 MHz, $CDCl_3$, δ, ppm): 178.76, 177.26, 160.52, 156.31, 152.06, 148.51, 147.32, 147.07, 145.23, 141.69, 141.54, 139.68, 137.90, 136.34, 135.44, 135.04, 134.11, 133.59, 132.85, 132.07, 131.93, 131.69, 131.36, 131.28, 131.15, 130.98, 130.55, 130.04, 129.77, 128.97, 128.91, 128.78, 128.72, 128.49, 127.90, 127.73, 127.08, 126.65, 126.60, 126.49, 126.37, 125.95, 125.53, 125.05, 124.98, 124.69, 124.48, 123.97, 123.36, 122.87, 122.62, 122.45, 122.42, 121.65, 121.26, 120.94, 120.41, 120.20, 119.51, 117.75, 117.29, 110.93, 110.03, 35.43, 31.23, 21.26. HR EI-MS: Calcd. for $[C_{83}H_{58}IrN_6S_2]^+$, 1395.38; Found, 1395.3788.

$[(CF_3\text{-}bt)_2Ir(L)](PF_6)$: The preparation of the complex **$[(CF_3\text{-}bt)_2Ir(L)](PF_6)$** was similar to that described for the complex **$[(nbt)_2Ir(L)](PF_6)$**, which was obtained from the reaction between the chloro-bridged dimer **$(CF_3\text{-}bt)_2Ir(\mu\text{-}Cl)_2Ir(CF_3\text{-}bt)_2$** (0.24 g, 0.15 mmol) and L (0.20 g, 0.30 mmol). The crude was purified by chromatography on silica gel using ethyl acetate/petroleum ether (1:1, v/v) as the eluent to give pale yellow powdery **$[(CF_3\text{-}bt)_2Ir(L)](PF_6)$** in 39.4 % yield (0.19 g). ^{1}H NMR (600 MHz, $CDCl_3$, δ, ppm): 8.66 (d, *J* = 8.4 Hz, 1H, Ar-H), 8.56 (d, *J* = 8.4 Hz, 1H, Ar-H), 8.31 (dd, *J* = 8.4, 7.8 Hz, 3H, Ar-H), 8.18 (s, 1H, Ar-H), 8.09 (d, *J* = 7.2 Hz, 1H, Ar-H), 8.06-7.95 (m, 5H, Ar-H), 7.87 (d, *J* = 8.4 Hz, 1H, Ar-H), 7.8 (dd, *J* = 7.8, 7.8 Hz, 3H, Ar-H), 7.44-7.39 (m, 6H, Ar-H), 7.35-7.29 (m, 7H, Ar-H), 7.25-7.22 (m, 4H, Ar-H), 7.09 (t, *J* = 8.8 Hz, 1H, Ar-H), 7.03-6.99 (m, 2H, Ar-H), 6.90 (d, *J* = 8.4 Hz, 1H, Ar-H), 6.74 (t, *J* = 7.8 Hz, 1H, Ar-H), 6.62 (d, *J* =

7.8 Hz, 1H, Ar-H), 6.46 (dd, *J* = 7.8, 8.4 Hz, 2H, Ar-H), 6.15 (d, *J* = 7.8 Hz, 1H, Ar-H), 2.48 (s, 3H, Ar-CH_3), 1.51 (s, 9H, -CH_3). ^{13}C NMR (150 MHz, $CDCl_3$, δ, ppm): 184.64, 182.65, 156.39, 152.14, 151.79, 151.56, 150.62, 148.17, 146.60, 145.29, 141.78, 140.36, 138.00, 135.11, 133.79, 133.31, 133.17, 132.91, 132.68, 131.49, 131.34, 130.61, 130.42, 130.16, 129.32, 129.08, 128.45, 128.12, 127.35, 126.75, 126.10, 125.48, 125.07, 124.74, 124.44, 124.16, 124.06, 123.86, 123.41, 123.09, 122.83, 122.69, 122.38, 122.03, 121.34, 120.63, 120.41, 120.09, 118.62, 117.94, 110.95, 110.21, 35.23, 31.21, 21.02. HR EI-MS: Calcd. for $[C_{77}H_{52}F_6IrN_6S_2]^+$, 1431.32; Found, 1431.3251.

2.3 Crystallography

Suitable single crystal of the ancillary ligand **L** was obtained from its methanol solution, whereas the single crystal of the cationic Ir(III) complex **$[(nbt)_2Ir(L)](PF_6)$** was obtained by the vapor diffusion of diethyl ether into its dichloromethane solution. The diffraction data were collected with a Bruker Smart Apex CCD diffractometer equipped with graphite-monochromatic Mo *K*α radiation (λ = 1.54178 Å or λ = 0.71073 Å) at 293(2) or 298(2) K. The structures were solved by direct methods and refined by full-matrix least-squares method on F^2 using SHELXL. All hydrogen atoms were added theoretically.

3. Results and discussion

3.1 Synthesis and characterization

The synthesis of the cationic Ir(III) complexes from Scheme 1 began first with preparing the ancillary ligand **L**. The ligand **L** was successfully obtained through five step reactions. First, the N-arylation of carbazole precursor was synthesized by the reaction of carbazole with 4-iodotoluene in high yield, and then further processed by using 1.10 equivalent of NBS to produce the

brominated intermediate. The brominated intermediate was converted into its arylboronic ester **I**. The intermediate **II** was Suzuki coupling reaction of the arylboronic ester **I** with 5-bromopicolinaldehyde. Finally, in the presence of ammonium acetate, the target **L** was prepared *via* reacting the intermediate **II** with phenanthrene-9,10-dione and 4-(tert-butyl)aniline in refluxing acetic acid. The ligand **L** was purified by column chromatography to give the pure product, and characterized using ^{1}HNMR, MS and X-ray crystallography.

The cationic Ir(III) complexes **[(nbt)$_2$Ir(L)](PF$_6$)** and **[(CF$_3$-bt)$_2$Ir(L)](PF$_6$)** were synthesized by reacting the corresponding Ir(III) chloro-bridged dimers with the ancillary ligand **L**, and followed by a counter ion-exchange reaction from Cl^- to PF_6^-. The two Ir(III) complexes were structurally characterized by ^{1}H NMR and the high resolution electro spray ionization mass spectra (HR ESI-MS), and the structure of **[(nbt)$_2$Ir(L)](PF$_6$)** was confirmed by X-ray crystallography.

The crystal structure and packing diagram of **L** is given in Fig. 1. The corresponding crystallographic data are summarized in Table 1. The crystal of **L** belongs to the triclinic space group P-1, a = 9.0069(5) Å, b = 11.0409(6) Å, c = 19.3194(12) Å, α = 74.556(2)°, β = 87.910(3)°, γ = 82.95(2)°, U = 1837.81(18) Å^3, Z = 2, D_c = 1.234 g/cm^3, μ = 0.557 mm^{-1}. As shown in Fig. 1(a), the pyridine ring is not coplanar with the adjacent carbazole ring, and the dihedral angle is 29.48^o. While the pyridine ring is nearly coplanar with the adjacent phenanthroimidazole skeleton, the dihedral angle is 3.49^o. The dihedral angle between carbazole ring and phenanthroimidazole skeleton is 30.0^o. In N-arylation of carbazole moiety, the dihedral angle between the benzene ring and the carbazole ring is 50.77^o. In N-arylation of phenanthroimidazole moiety, the benzene ring is nearly perpendicular to the phenanthroimidazole skeleton, and the dihedral angle is 89.18^o. From its

packing diagram (Fig. 1(b)), it is found that there is strong intermolecular π–π interaction between two anti-paralleled molecules in a unit crystal cell, the interplanar distance is about 3.637 Å. However the intermolecular interactions are disconnected between different unit cells in the crystal lattices and thus no intermolecular π–π stacking exist in **L** crystal.

The crystal structure of **[(nbt)$_2$Ir(L)](PF$_6$)** is shown in Fig. 2. Its corresponding crystallographic data is given in Table 1, and the selected bond lengths and angles are listed in Table 2. The crystal of **[(nbt)$_2$Ir(L)](PF$_6$)** also belongs to the triclinic space group P-1, a = 15.6730(13) Å, b = 16.5860(14) Å, c = 16.9220(14) Å, α = 94.2760(10)°, β = 111.502(3)°, γ = 103.676(2)°, U = 3913.0(6) Å^3, Z = 2, D_c = 1.308 g/cm^3, μ = 1.840 mm^{-1}. From Fig. 2, it was found that the coordination center of iridium(III) is surrounded by two N atoms and two C atoms from the cyclometalated ligands (**nbt**, i.e. C^N ligand) and two N atoms from the ancillary ligand **L** (N^N ligand), and the iridium(III) center adopts a distorted octahedral coordination geometry. Two C atoms and two N atoms from the cyclometalated ligands exhibit *cis-C,C* and *trans-N,N* chelate mode, and two N atoms from the ligand **L** locate *cis-N,N* chelate disposition. Moreover, it can be seen from Table 2 that the distances of Ir-C (C^N ligand) bonds (2.021(7) and 1.968(8) Å) are slightly shorter than the Ir-N (C^N ligand) bonds (2.066(5) and 2.068(5) Å). The Ir-N (N^N ligand) distances (2.239(6) and 2.175(5) Å) are longer than the distances of Ir-N (C^N ligand).

3.2 Photophysical, electrochemical and thermal properties of the cationic Ir(III) complexes

The UV-vis absorption spectra of the free ligands and the complexes, and the photoluminescence spectra of the ligand **L** and the complexes **[(nbt)$_2$Ir(L)](PF$_6$)** and **[(CF$_3$-bt)$_2$Ir(L)](PF$_6$)** in degassed dichloromethane solution are shown in Fig. 3. As shown in Fig.

3, the absorption bands of the free ligands mainly located below 400 nm. The ligand L exhibits four intense absorption bands at 260, 295, 348 and 368 nm, while the ligands **nbt** and **CF_3-bt** only show one intense absorption band at 320 and 290 nm, respectively. These absorption bands of the free ligands could be attributed to the π–π* transitions. In addition, with increasing the π-conjugation of the ligand (**L**>**nbt**>**CF_3-bt**), the longwave absorption bands of **nbt** and **L** were red-shifted by about 30 and 78 nm, respectively, compared to the ligand **CF_3-bt**. For the two cationic Ir(III) complexes, the intense absorption bands before 300 nm in their absorption spectra are assigned to the spin-allowed ^{1}(π–π*) ligand-centered transition of the cyclometalated primary ligand and the ancillary ligand in the complexes. The following relatively weak absorption band at 352 nm for **$[(nbt)_2Ir(L)](PF_6)$** could be attributed to both spin-allowed metal-to-ligand charge-transfer (^{1}MLCT) and ligand-to-ligand charge-transfer (^{1}LLCT) transitions, while that for **$[(CF_3\text{-}bt)_2Ir(L)](PF_6)$** is blue-shifted to 327 nm due to an electron withdrawing group (-CF_3) attached in its primary ligand. Moreover, the weaker absorption bands that found at lower energy region ranging from 400 to 500 nm in the absorption spectra of the Ir(III) complexes are attributed to the spin-forbidden ^{3}MLCT and ^{3}LLCT [37-39]. Table 3 summarized the photophysical data of the two cationic Ir(III) complexes.

From Fig. 3, under ultraviolet light excitation, the ligand **L** displays bright blue emission with peak at 430 nm in dilute solution. Under the excitation of 427 nm, the complex **$[(nbt)_2Ir(L)](PF_6)$** exhibits red emission with a maximum peak at 601 nm and a shoulder peak at 651 nm in degassed dichloromethane solution at room temperature, while the complex **$[(CF_3\text{-}bt)_2Ir(L)](PF_6)$** shows orange emission with a maximum peak at 579 nm. The CIE coordinates of **$[(nbt)_2Ir(L)](PF_6)$** and

[$(CF_3$-bt$)_2$Ir(L)](PF$_6$) are (0.627, 0.370) and (0.495, 0.494), respectively. Compared with the similar Ir(III) complex (CF_3-bt$)_2$Ir(acac) (λ_{em} = 554 nm) [36], the maximum emission peak of **[$(CF_3$-bt$)_2$Ir(L)](PF$_6$)** was red-shifted by about 25 nm. It could be that varying the ancillary ligand from acac to pyridylbenzimidazole in the octahedral Ir(III) system led to a lowering of the ^{3}MLCT energy gap, giving a change from yellow to orange emission. In addition, the photoluminescence quantum yields of **[$(nbt)_2$Ir(L)](PF$_6$)** and **[$(CF_3$-bt$)_2$Ir(L)](PF$_6$)** at room temperature were measured to be 5.51% and 1.72% in dichloromethane solution (ca. 10^{-6} mol/L) through an absolute method using the Edinburgh Instruments spectrometer (FLS920) integrating sphere excited at 427 nm with a Xe lamp.

The phosphorescence lifetime (τ) is the crucial factor that determines the rate of triplet-triplet annihilation in OLEDs, and the longer τ values usually cause greater triplet-triplet annihilation [40]. The photoluminescence decay lifetimes of **[$(nbt)_2$Ir(L)](PF$_6$)** and **[$(CF_3$-bt$)_2$Ir(L)](PF$_6$)** in dichloromethane solution were measured to be 1.10 μs and 1.40 μs with a time-correlated single photon counting spectrometer using an Edinburgh Instruments spectrometer (FLS920) with a microsecond flash lamp as the excitation source (repetition rate 90 Hz) at room temperature.

In order to investigate the frontier orbitals of the cationic Ir(III) complexes, cyclic voltammetry (CV) was carried out to investigate their electrochemical behavior. Their HOMO (highest occupied molecular orbital) energy levels were calculated from the onset of the oxidation potentials of their cyclic voltammetry measurements, while their LUMO (lowest unoccupied molecular orbital) energy levels were deduced from their HOMO energy levels and optical band gaps determined from their extrapolated UV-Vis absorption edges [41]. The cyclic voltammograms of **[$(nbt)_2$Ir(L)](PF$_6$)**

and **[$(CF_3$-bt$)_2$Ir(L)](PF$_6$)** were measured in degassed dichloromethane solution with Bu_4NPF_6 (0.1 mol/L) as the electrolyte (Fig. 4). A platinum working electrode and a saturated Ag/AgCl reference electrode were used. Ferrocene was used for potential calibration. As shown in Fig. 4, the first oxidation potentials of **[(nbt)$_2$Ir(L)](PF$_6$)** and **[$(CF_3$-bt$)_2$Ir(L)](PF$_6$)** were at ca.1.43 and 1.45 V, respectively. Under the same conditions, the oxidation and reduction potentials of ferrocene were observed at 0.43 and 0.31 V, respectively, then the $E_{1/2}$ (Fc/Fc^+) is 0.37 V. Thus, the HOMO energy levels of **[(nbt)$_2$Ir(L)](PF$_6$)** and **[$(CF_3$-bt$)_2$Ir(L)](PF$_6$)** were calculated to be -5.86 and -5.88 eV, regarding the energy level of ferrocene/ferrocenium as -4.80 eV. The optical band edges of **[(nbt)$_2$Ir(L)](PF$_6$)** and **[$(CF_3$-bt$)_2$Ir(L)](PF$_6$)** were estimated to be at ca. 502 and 482 nm, which corresponds to 2.47 and 2.57 eV. Therefore, the LUMO energy levels of **[(nbt)$_2$Ir(L)](PF$_6$)** and **[$(CF_3$-bt$)_2$Ir(L)](PF$_6$)** were calculated to be -3.39 and -3.31 eV, respectively.

The thermal properties of the cationic Ir(III) complexes were investigated using thermogravimetric analysis (TGA) under a nitrogen atmosphere. The results of their TGA measurements are shown in Fig. 5. From their TGA curves in Fig. 5, **[(nbt)$_2$Ir(L)](PF$_6$)** and **[$(CF_3$-bt$)_2$Ir(L)](PF$_6$)** exhibited good thermal stability up to 320 ^oC (< 3% weight loss), with increasing temperature, **[(nbt)$_2$Ir(L)](PF$_6$)** and **[$(CF_3$-bt$)_2$Ir(L)](PF$_6$)** began to decompose at 360 ^oC accompanied by a sharp weight loss in their TGA curves. The result indicates that the Ir(III) complexes are potential emitting material for the fabrication of stable OLEDs.

4. Conclusion

In summary, two novel cationic iridium(III) complexes with phenanthroimidazole derivative as

the ancillary ligand were synthesized and characterized. The cationic iridium(III) complexes exhibit high thermal stability, and display strong red and orange emissions with photoluminescence quantum efficiency of 5.51% and 1.72%, respective, suggesting that they are potential emitting materials for the fabrication of stable OLEDs.

Appendix A. Supplementary data

CCDC 1556705 and 1563488 contain the supplementary crystallographic data for the ancillary ligand **L** and the complex **$[(nbt)_2Ir(L)](PF_6)$** in this paper. These data can be obtained free of charge via http:www.ccdc.cam.ac.uk/conts/retrieving.html, or from the Cambridge Crystallographic Data Centre, 12 Union Road, Cambridge CB2 1EZ, UK; fax: (+44) 1223-336-033; or e-mail: deposit@ccdc.cam.ac.uk.

Electronic supplementary information (ESI) available: the 1H, 13C NMR and mass spectra for the synthesized L and Ir(III) complexes.

Acknowledgements

This work was supported by the National Natural Science Foundation of China (Grant 51563014).

References

[1] H. Yersin, Highly efficient OLEDs with phosphorescent materials, Wiley-VCH, Weinheim, 2008.

[2] W.-Y. Wong, C.-L. Ho, Heavy metal organometallic electrophosphors derived from multi-component chromophores, Coord. Chem. Rev., 2009, 253, 1709−1758.

[3] C.-L. Ho, B. Yao, B.H. Zhang, K.-L. Wong, W.-Y. Wong, Z.Y. Xie, L.X. Wang, Z.Y. Lin, Metallophosphors of iridium(III) containing borylated oligothiophenes with electroluminescence down to the near-infrared region, J. Organomet. Chem., 2013, 730, 144−155.

[4] Y. Chi, P.-T. Chou, Transition-metal phosphors with cyclometalating ligands: fundamentals and applications, Chem. Soc. Rev., 2010, 39, 638−655.

[5] L.X. Xiao, Z.J. Chen, B. Qu, J.X. Luo, S. Kong, Q.H. Gong, J. Kido, Recent Progresses on Materials for Electrophosphorescent Organic Light-Emitting Devices, Adv. Mater., 2011, 23, 926−952.

[6] G.J, Zhou, W.-Y. Wong, B. Yao, Z.Y. Xie, L.X. Wang, Triphenylamine-dendronized pure red iridium phosphors with superior OLED efficiency/color purity trade-offs, Angew. Chem. Int. Ed., 2007, 46, 1149−1151.

[7] T.Z. Yu, Y.L. Shi, H.F. Chai, L.X. Niu, P. Liu, Y.L. Zhao, J.D. Kang, B. Gao, H. Zhang, Synthesis, characterization, and photo- and electro-luminescence of Ir(III) complexes containing carrier transporting group-substituted β-diketonate ligand, RSC Adv., 2014, 4, 11680−11688.

[8] T.Z. Yu, Y. Cao, W.M. Su, C.C. Zhang, Y.L. Zhao, D.W. Fan, M.J. Huang, K. Yue, S.Z.D. Cheng, Synthesis, structure, photo- and electro-luminescence of an iridium(III) complex with novel carbazole functionalized β-diketone ligand, RSC Adv., 2014, 4, 554−562.

[9] T.Z. Yu, Z.X. Xu, W.M. Su, Y.L. Zhao, H. Zhang, Y.J. Bao, Highly efficient phosphorescent materials based on Ir(III) complexes-grafted on a polyhedral oligomeric silsesquioxane core, Dalton Trans., 2016, 45, 13491−13502.

[10] C. Adachi, M.A. Baldo, M.E. Thompson, S.R. Forrest, Nearly 100% internal phosphorescence efficiency in an organic light-emitting device, J. Appl. Phys. 2001, 90, 5048−5051.

[11] M.A. Baldo, S. Lamansky, P.E. Burrows, M.E. Thompson, S.R. Forrest, Very high-efficiency green organic light-emitting devices based on electrophosphorescence, Appl. Phys. Lett. 1999, 75, 4−6.

[12] M. Ikai, S. Tokito, Y. Sakamoto, T. Suzuki, Y. Taga, Highly efficient phosphorescence from organic light-emitting devices with an exciton-block layer, Appl. Phys. Lett. 2001, 79, 156−158.

[13] Y.M. You, S. Cho, W. Nam, Cyclometalated iridium(III) complexes for phosphorescence sensing of biological metal ions, Inorg. Chem., 2014, 53, 1804−1815.

[14] C.D. Sunesh, G. Mathai, Y. Choe, Constructive effects of long alkyl chains on the electroluminescent properties of cationic iridium complex-based light-emitting electrochemical cells, ACS Appl. Mater. Interfaces, 2014, 6, 17416−17425.

[15] L. He, L. Duan, J. Qiao, G.F. Dong, L.D. Wang, Y. Qiu, Highly efficient blue-green and white light-emitting electrochemical cells based on a cationic iridium complex with a bulky side group, Chem. Mater., 2010, 22, 3535–3542.

[16] R.D. Costa, E. Ortí, H.J. Bolink, S. Graber, S. Schaffner, M. Neuburger, C.E. Housecroft, E.C. Constable, Archetype cationic iridium complexes and their use in solid-state light-emitting electrochemical cells, Adv. Funct. Mater., 2009, 19, 3456–3463.

[17] H.J. Tang, Y.H. Li, Q.L. Chen, B. Chen, Q.Q. Qiao, W. Yang, H.B. Wu, Y. Cao, Efficient yellow-green light-emitting cationic iridium complexes based on 1,10-phenanthroline derivatives containing oxadiazole-triphenylamine unit, Dyes and Pigments, 2014, 100, 79–86.

[18] R. Tao, J. Qiao, G.L. Zhang, L. Duan, L.D. Wang, Y. Qiu, Efficient near-infrared-emitting cationic iridium complexes as dopants for OLEDs with small efficiency roll-off, J. Phys. Chem. C, 2012, 116, 11658−11664.

[19] N.Z. Luo, Y. Lan, R.R. Tang, L. He, L. Duan, A cationic iridium complex meets an electron-transporting counter-anion: enhanced performances for solution-processed phosphorescent light-emitting diodes, Chem. Commun., 2016, 52, 14466−14469.

[20] B. Chen, Y.H. Li, Y.Y. Chu, A.M. Zheng, J.W. Feng, Z.T. Liu, H.B. Wu, W. Yang, Highly efficient single-layer organic light-emitting devices using cationic iridium complex as host, Org. Electronics, 2013, 14, 744–753.

[21] T. Hu, L. He, L. Duan, Y. Qiu, Solid-state light-emitting electrochemical cells based on ionic iridium(III) complexes, J. Mater. Chem., 2012, 22, 4206–4215.

[22] J.D. Slinker, A.A. Gorodetsky, M.S. Lowry, J. Wang, S. Parker, R. Rohl, S. Bernhard, G.G. Malliaras, Efficient yellow electroluminescence from a single layer of a cyclometalated iridium complex, J. Am. Chem. Soc., 2004, 126, 2763–2767.

[23] Y.L. Shen, D.D. Kuddes, C.A. Naquin, T.W. Hesterberg, C. Kusmierz, B.J. Holliday, J.D. Slinker, Improving light-emitting electrochemical cells with ionic additives, Appl. Phys. Lett., 2013, 102, 203305.

[24] W.Y. Wong, G.J. Zhou, X.M. Yu, H.S. Kwok, Z. Lin, Efficient organic light-emitting diodes based on sublimable charged iridium phosphorescent emitters, Adv. Funct. Mater., 2007, 17, 315–323.

[25] C. Wu, H.F. Chen, K.T. Wong, M.E. Thompson, Study of ion-paired iridium complexes (soft salts) and their application in organic light emitting diodes, J. Am. Chem. Soc., 2010, 132, 3133–3139.

[26] G. Nasr, A. Guerlin, F. Dumur, L. Beouch, E. Dumas, G. Clavier, F. Miomandre, F. Goubard, D. Gigmes, D. Bertin, G. Wantze, C.R. Mayer, Iridium(iii) soft salts from dinuclear cationic and mononuclear anionic complexes for OLED devices, Chem. Commun., 2011, 47, 10698–10700.

[27] D.X. Ma, C. Zhang, Y. Qiu, L. Duan, Highly efficient blue-green organic light-emitting diodes achieved by controlling the anionic migration of cationic iridium(iii) complexes, J. Mater. Chem. C, 2016, 4, 5731–5738.

[28] D.X. Ma, T. Tsuboi, Y. Qiu, L. Duan, Recent progress in ionic iridium(III) complexes for organic electronic devices, Adv. Mater., 2017, 29, 1603253.

[29] T. M^{c}Cormick, W.L. Jia, S. Wang, Phosphorescent Cu(I) complexes of 2-(2'-pyridylbenzimidazolyl)benzene: Impact of phosphine ancillary ligands on electronic and photophysical properties of the Cu(I) complexes, Inorg. Chem., 2006, 45, 147-155.

[30] B.H. Kim, D.N. Lee, H.J. Park, J.H. Min, Y.M. Jun, S.J. Park, W.Y. Lee, Synthesis and characterization of electrochemiluminescent ruthenium(II) complexes containing *o*-phenanthroline and various α-diimine ligands, Talanta, 2004, 62, 595–602.

[31] T. Lazarides, M.A.H. Alamiry, H. Adams, S.J.A. Pope, S. Faulkner, J.A. Weinstein, M.D. Ward, Anthracene as a sensitiser for near-infrared luminescence in complexes of Nd(III), Er(III) and Yb(III): an unexpected sensitisation mechanism based on electron transfer, Dalton Trans., 2007, 1484–1491.

[32] T.Z. Yu，H.F. Chai, Y.L. Zhao, C.C. Zhang, P. Liu, D.W. Fan, Synthesis, crystal structure and photoluminescence of phosphorescent copper(I) complexes containing hole-transporting carbazoly moiety, Spectrochim. Acta Part A, 2013, 109, 179–185.

[33] T.Z. Yu, P. Liu, H.F. Chai, J.D. Kang, Y.L. Zhao, H. Zhang, D.W. Fan, Synthesis, crystal structures and photo- and electro-luminescence of copper(I) complexes containing electron-transporting diaryl-1,3,4-oxadiazole, J. Fluoresc., 2014, 24, 933–943.

[34] T.Z. Yu, R.Z. Liang, Y.L. Zhao, Y.L. Song, B. Gao, M.H. Li, L.F. Min, H. Zhang, D.W. Fan, Gadolinium, terbium and europium complexes containing dibenzoylmethane and carbazole-functionalized 2-(2-pyridyl)-benzimidazole: Structural and spectroscopic characterization, Polyhedron, 2015, 85, 789–794.

[35] T.Z. Yu, Y.J. Bao, Y.L. Zhao, H. Zhang, Z.X. Xu and X.M. Wu, Synthesis, photo- and electro-luminescence of red-emitting Ir(III)complexes with 2-(1-naphthyl) benzothiazole and carrier transporting group-functionalized picolinate ligands, J. Organomet. Chem., 2016, 825–826, 33–40.

[36] R.J. Wang, D. Liu, H.C. Ren, T. Zhang, H.M. Yin, G.Y. Liu, J.Y. Li, Highly efficient orange and white organic light-emitting diodes based on new orange iridium complexes, Adv. Mater., 2011, 23, 2823–2827.

[37] S.F. Huang, H.Z. Sun, G.G. Shan, F.S. Li, Q.Y. Zeng, K.Y. Zhao, Z.M. Su, Rational design and synthesis of cationic Ir(III) complexes with triazolate cyclometalated and ancillary ligands for multi-color tuning, Dyes and Pigments, 2017, 139, 524–532.

[38] W.Y. Wong, G.J. Zhou, X.M. Yu, H.S. Kwok, B.Z. Tang, Amorphous diphenylaminofluorene-functionalized iridium complexes for high-efficiency electrophosphorescent light-emitting diodes, Adv. Funct. Mater., 2006, 16, 838–846.

[39] S. Bettington, M. Tavasli, M.R. Bryce, A. Beeby, H. Al-Attar, A.P. Monkman, Tris-cyclometalated iridium (III) complexes of carbazole(fluorenyl)pyridine ligands: Synthesis, redox and photophysical properties, and electrophosphorescent light-emitting diodes, Chem. Eur. J., 2007, 13, 1423–1431.

[40] M.A. Baldo, S.R. Forrest, Transient analysis of organic electrophosphorescence: I. Transient analysis of triplet energy transfer, Phys. Rev. B, 2000, 62, 10958–10966.

[41] P. Brulatti, R.J. Gildea, J.A.K. Howard, V. Fattori, M. Cocchi, J.A.G. Williams, Luminescent iridium(III) complexes with N^C^N-coordinated terdentate ligands: Dual tuning of the emission energy and application to organic light-emitting devices, Inorg. Chem., 2012, 51, 3813–3826.

Legends

Scheme 1. Synthetic routes of the ligand (**L**) and the Ir(III) complexes.

Fig. 1. Crystal structure (a) and packing diagram (b) of **L**.

Fig. 2. Crystal structure of **[(nbt)$_2$Ir(L)](PF$_6$)**.

Fig. 3. Normalized UV-vis absorption spectra of the free ligands and the complexes, and photoluminescence spectra of the ligand **L** and the complexes **[(nbt)$_2$Ir(L)](PF$_6$)** and **[(CF$_3$-bt)$_2$Ir(L)](PF$_6$)** in degassed CH_2Cl_2 solution at room temperature. (C = 1.0×10^{-5} mol/L, λ_{ex} = 427 nm for **[(nbt)$_2$Ir(L)](PF$_6$)** and **[(CF$_3$-bt)$_2$Ir(L)](PF$_6$)**)

Fig. 4. Cyclic voltammograms of ferrocene, **[(nbt)$_2$Ir(L)](PF$_6$)** and **[(CF$_3$-bt)$_2$Ir(L)](PF$_6$)** (Scan rate: 10 mV/s; solvent: dichloromethane).

Fig. 5. Thermogravimetric analyses (TGA) of **[(nbt)$_2$Ir(L)](PF$_6$)** and **[(CF$_3$-bt)$_2$Ir(L)](PF$_6$)** in nitrogen atmosphere (heating rate: 10 ^{o}C/min).

Table 1. Crystallographic data for **L**

Table 2. Selected bond lengths and bond angles for **[(nbt)$_2$Ir(L)](PF$_6$)**

Table 3. Photophysical, thermal and electrochemical properties of the cationic Ir(III) complexes

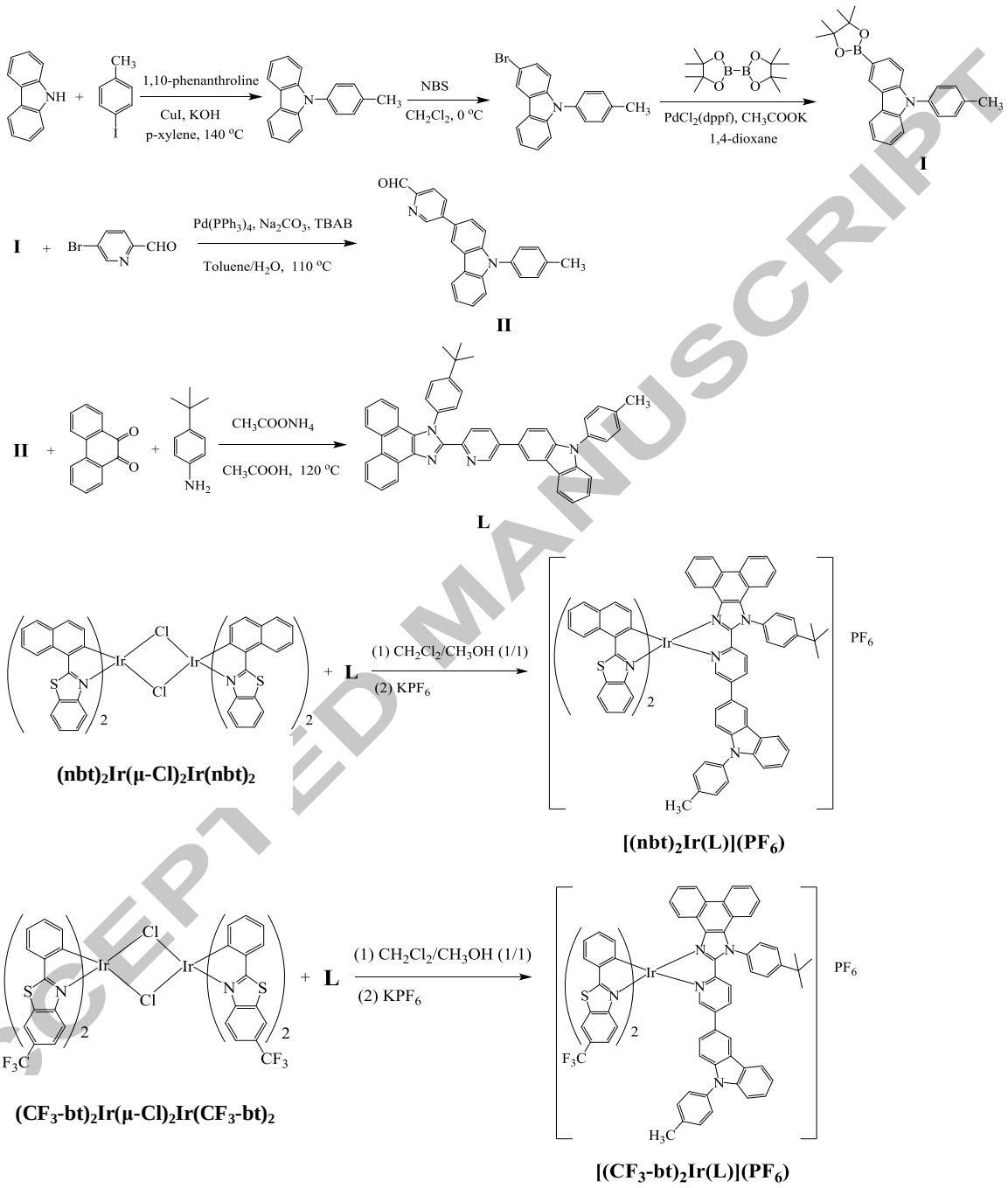

Scheme 1

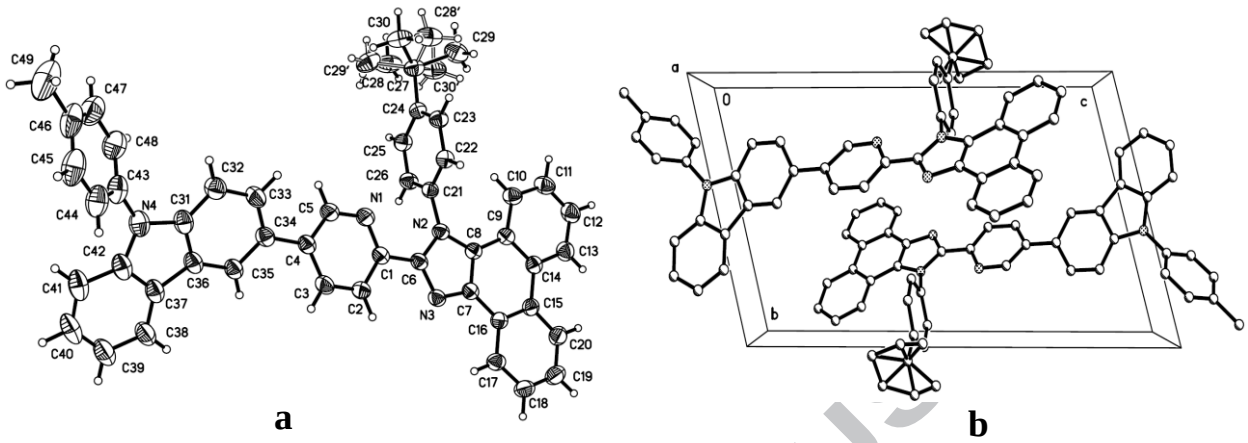

Fig. 1

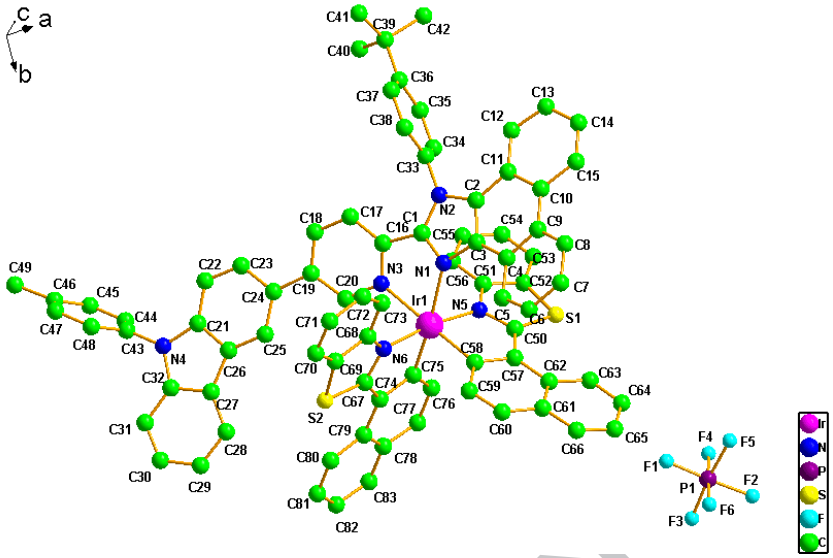

Fig. 2

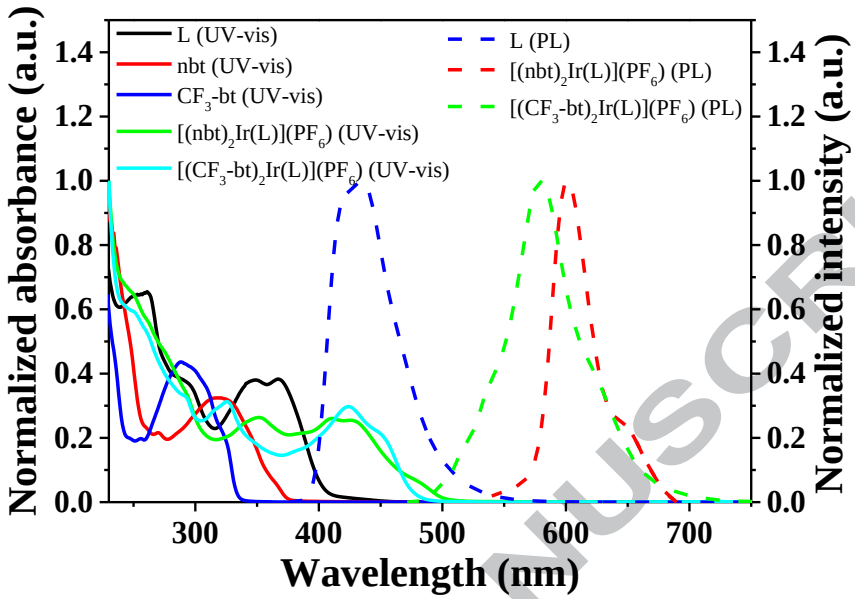

Fig. 3

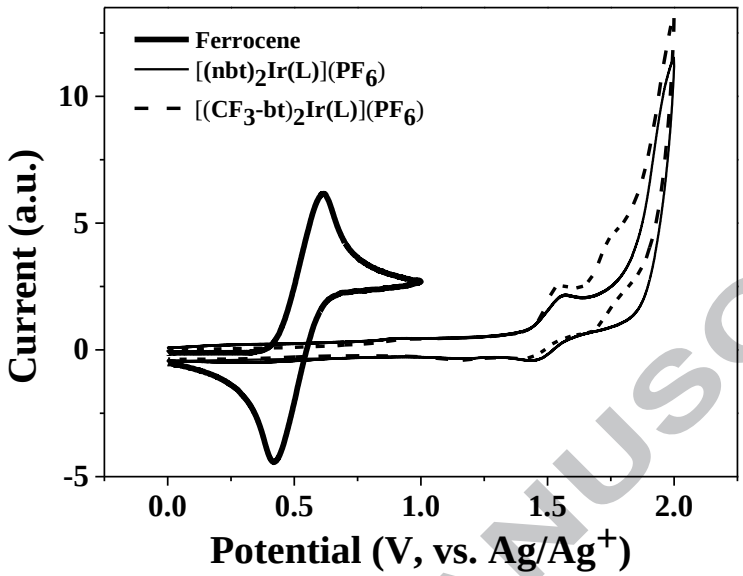

Fig. 4

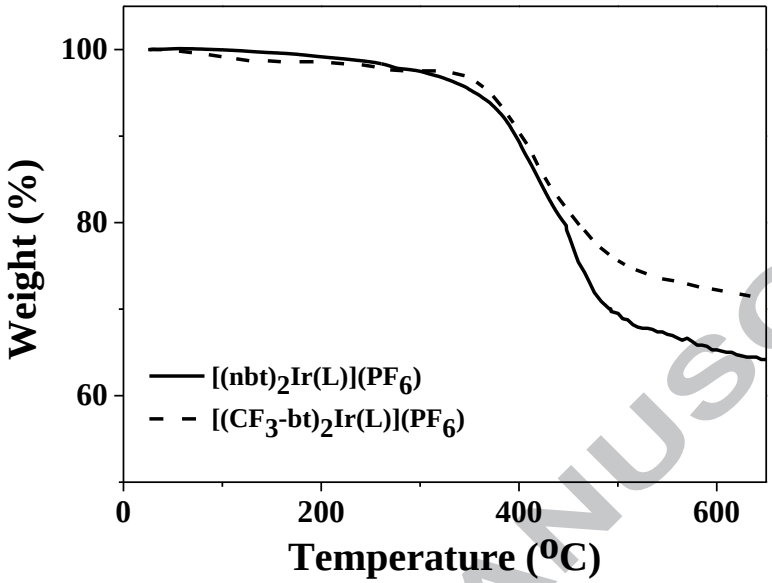

Fig. 5

Table 1. Crystallographic data for **L** and **$[(nbt)_2Ir(L)](PF_6)$**

Compound	**L**	**$[(nbt)_2Ir(L)](PF_6)$**
Empirical formula	$C_{49}H_{38}N_4$	$C_{83}H_{58}F_6IrN_6PS_2$
Formula weight	682.83	1540.64
Temperature (K)	293(2)	298(2)
Wavelength (Å)	1.54178	0.71073
Crystal system	Triclinic	Triclinic,
Space group	P-1	P-1
Unit cell dimensions		
a (Å)	9.0069(5)	15.6730(13)
b (Å)	11.0409(6)	16.5860(14)
c (Å)	19.3194(12)	16.9220(14)
α (°)	74.556(2)	94.2760(10)
β (°)	87.910(3)	111.502(3)
γ (°)	82.95(2)	103.676(2)
Volume ($Å^3$), Z	1837.81(18), 2	3913.0(6), 2
Density (calculated) (g/cm^3)	1.234	1.308
Absorption coefficient (mm^{-1})	0.557	1.840
F (000)	720	1552
Crystal size (mm)	0.21 × 0.14 × 0.08	0.27 × 0.18 × 0.10
θ range for data collected (°)	4.18 ─ 66.02	2.31 ─ 25.02
Limiting indices	$-9 \le h \le 10$, $-10 \le k \le 13$, $-21 \le l \le 22$	$-18 \le h \le 13$, $-18 \le k \le 19$, $-19 \le l \le 20$
Reflections collected	12268	20004
Independent reflections	6403 (R_{int} = 0.0279)	13573 (R_{int} = 0.0786)
Absorption correction	Semi-empirical from equivalents	Semi-empirical from equivalents
Max. and min. transmission	0.9568 and 0.8919	0.8374 and 0.6365
Refinement method	Full-matrix least-squares on F^2	Full-matrix least-squares on F^2
Data / restraints / parameters	6403 / 0 / 513	13573 / 0 / 896
Goodness-of-fit on F^2	1.091	1.064
Final R indices [I > 2σ (I)]	R_1 = 0.0527, wR_2 = 0.1210	R_1 = 0.0644, wR_2 = 0.1450
R indices (all data)	R_1 = 0.0914, wR_2 = 0.1352	R_1 = 0.0889, wR_2 = 0.1514
Largest diff. Peak and hole ($eÅ^{-3}$)	0.186 and -0.213	1.499 and -1.188

Table 2. Selected bond lengths and bond angles for **$[(nbt)_2Ir(L)](PF_6)$**

Bond length (Å)			
Ir(1)–N(1)	2.239(6)	Ir(1)–N(3)	2.175(5)
Ir(1)–N(5)	2.066(5)	Ir(1)–N(6)	2.068(5)
Ir(1)–C(58)	2.021(7)	Ir(1)–C(75)	1.968(8)
Bond angles (^{o})			
N(1)–Ir(1)–N(3)	74.1(2)	N(1)–Ir(1)–N(5)	82.7(2)
N(1)–Ir(1)–N(6)	103.9(2)	N(1)–Ir(1)–C(58)	103.9(2)
N(1)–Ir(1)–C(75)	171.1(2)	N(3)–Ir(1)–N(5)	102.6(2)
N(3)–Ir(1)–N(6)	84.2(2)	N(3)–Ir(1)–C(58)	177.4(2)
N(3)–Ir(1)–C(75)	98.0(2)	N(5)–Ir(1)–N(6)	171.7(2)
N(5)–Ir(1)–C(58)	78.6(2)	N(5)–Ir(1)–C(75)	95.4(3)
N(6)–Ir(1)–C(58)	94.8(2)	N(6)–Ir(1)–C(75)	78.8(3)
C(58)–Ir(1)–C(75)	84.1(3)		

Table 3. Photophysical, thermal and electrochemical properties of the cationic Ir(III) complexes

Complex	UV-vis (nm)	PL (nm)	T_d (^{o}C)	Φ_f (%)	τ (μs)	E_{OX} (V)	HOMO (eV)	LUMO (eV)
$[(nbt)_2Ir(L)](PF_6)$	251, 352, 411 427	601 651	360	5.51	1.10	1.43	-5.86	-3.39
$[(CF_3\text{-}bt)_2Ir(L)](PF_6)$	251, 327, 427	579	335	1.72	1.40	1.45	-5.88	-3.31

Graphical Abstract:

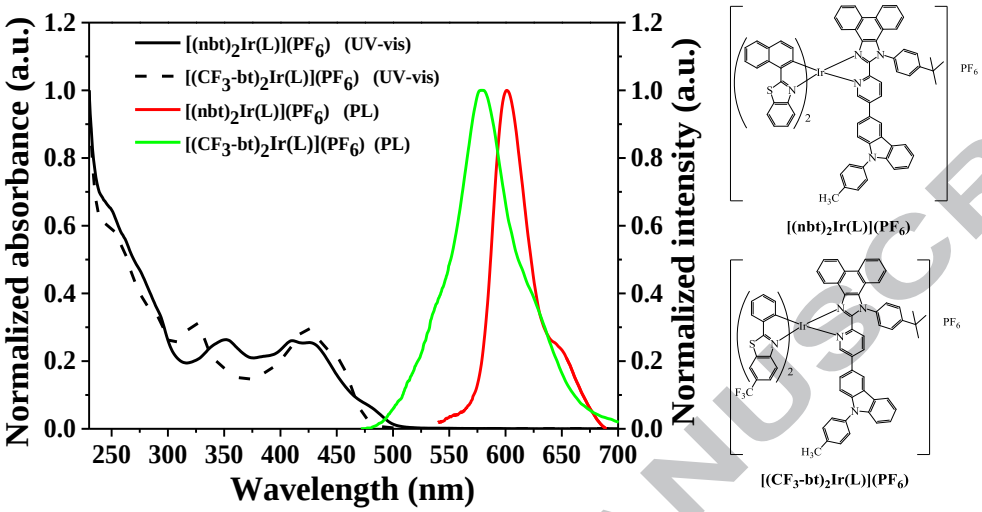

Graphical Abstract: Synopsis

Two novel cationic Ir(III) complexes were successfully synthesized and characterized, and their photophysical, electrochemical properties and thermal stabilities were investigated systematically.